ACADEMIA ROMÂNĂ
Revue Roumaine de Chimie
http://web.icf.ro/rrch/

Rev. Roum. Chim.,
2017, *62*(4-5), 399-412

Dedicated to Professor Ionel Haiduc
on the occasion of his 80th anniversary

COMPARATIVE STUDIES REGARDING THE IMPACT OF THE SYNTHESIS POSSIBILITIES ON THE PHYSICO-CHEMICAL PROPERTIES OF POLY(N,N-DIMETHYLAMINOETHYL METHACRYLATE)

Alina G. RUSU, Alina DIACONU, Nita TUDORACHI, Mihai ASANDULESA, Loredana E. NITA, Mihaela CRISTEA, Iordana NEAMTU and Aurica P. CHIRIAC*

"Petru Poni" Institute of Macromolecular Chemistry
41-A Grigore Ghica Voda Alley, 700487 Iaşi, Roumania

Received December 12, 2016

In this study the synthesis of poly(2-(dimethylamino) ethyl methacrylate) (PDMAEMA), via free radical polymerization by using three different variants of initiation namely azobis(isobutyronitrile) (AIBN), 4,4′-Azobis(4-cyanovaleric acid) (ACVA), and a redox system composed of potassium persulfate (KPS) and ascorbic acid (AscA), is presented. The structure and the molecular weight of the homopolymers, accordingly with the synthesis variant, were investigated by Fourier Transform Infrared Spectroscopy (FTIR) and static light scattering (SLS), respectively. The variation of the hydrodynamic diameter (D_h) of the PDMAEMA particles in relation with temperature was put into evidence by dynamic light scattering (DLS) technique. The PDMAEMA behavior during thermal degradation has been thoroughly investigated by thermogravimetry (TGA) coupled with FTIR and Mass Spectrometry (MS). In addition, the dielectric properties were put into evidence using a dielectric analyzer at different frequencies and temperatures. The dielectric spectroscopy study of the homopolymer samples showed that β-relaxation is localized at low temperatures, while a further increase of temperature α-relaxation connected to glass transition is recognized only at high frequencies.

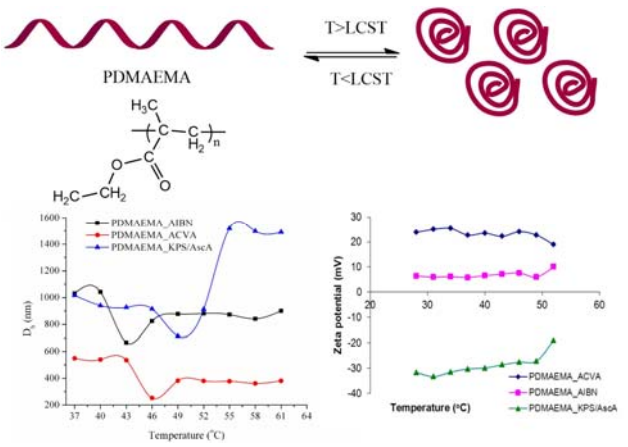

INTRODUCTION

Stimuli-responsive materials that undergo physical and chemical changes in response to external stimuli have received increasing attention due to their wide applications in nanomedicine, gene delivery and tissue engineering.[1] Specifically, one of the most commonly studied groups of smart materials with pH and temperature-responsiveness for biological applications are poly(N,N-dimethylaminoethyl methacrylate) (PDMAEMA)-based gels.[2] As reported in literature, PDMAEMA

* Corresponding author: achiriac1@yahoo.com

is a polycation with antibacterial, hemostatic and anticancer properties[3] that contains tertiary amino-groups which are positively charged in the acidic pH domain[4]; it has the pKa of about 7.5 which is close to the physiological pH[5] and lower critical solution temperature (LCST) at about 45°C at pH 8.5, and at pH 7.0 higher than 50°C [6]. Over the years, PDMAEMA and DMAEMA-containing copolymers have been evaluated both in solution and also as components of various systems (scaffolds, hydrogels[7], polyplexes[8]) with biomedical applications. The synthesis of PDMAEMA can be accomplished by free radical polymerization[9] and atom transfer radical polymerization (ATRP)[10]. In order to prepare polymers for bio-applications, radical polymerization has noteworthy advantages. The reaction conditions are generally not as challenging as in the case of ATRP reaction and it is possible to polymerize a diversity of monomers by radical polymerization. In this context, this study presents the PDMAEMA synthesis by radical polymerization using three variants of initiation systems namely 2,2′-Azobis(2-methylpropionitrile) (AIBN), 4,4′-Azobis(4-cyanopentanoic acid), (ACVA) and the redox system based on potassium persulfate (KPS) and ascorbic acid (AscA). Additionally, following the synthesis variants of the PDMAEMA, it was evaluated the influence of the initiation system upon the thermal stability, temperature-responsiveness, molecular weight and dielectric properties of the homopolymers.

RESULTS AND DISCUSSION

As it is well known PDMAEMA is part of the class of stimuli-responsive polymers with great potential for bio-applications as tissue regeneration, clinical diagnostics, drug delivery, and sensing. Thus, as pH-responsive polymer PDMAEMA exhibits a change in the ionization state upon variation of the pH leading it to conformational change, behavior that highlights its applicability as vector in drug delivery systems. Owing to these special characteristics offered by the homopolymer, various techniques were used for its preparation. In Table 1 are presented the radical active species which initiate the polymerization of N,N-dimethylaminoethyl methacrylate (DMAEMA) in this study. In the following it is presented the characterization of the homopolymer in relation with the variant initiation system.

Table 1

Active species initiating the polymerization of DMAEMA

Initiation system	Active species which initiate the polymerization
2,2′-Azobis(2-methylpropionitrile) (AIBN)	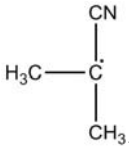 – 2-methylpropionitrile radicals
4,4′-Azobis(4-cyanopentanoic acid) (ACVA)	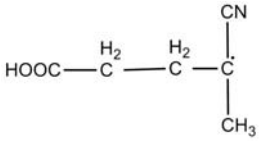 – 4-cyanopentanoic acid radicals
Potassium persulfate/Ascorbic acid (KPS/AscA)	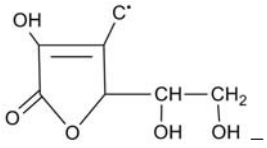 – ascorbate radicals $SO_4^{-\cdot}$ – sulphate ion radicals

FTIR spectroscopy

The FTIR spectra of the synthesized homopolymers accordingly with the initiation variant, respectively PDMAEMA_AIBN, PDMAEMA_ACVA and PDMAEMA_KPS/AscAs, are illustrated in Figure 1. A well-defined band at 1728 cm^{-1}, characteristic to the stretching vibration of C=O groups of esters was observed in the PDMAEMA_AIBN and PDMAEMA_ACVA spectra.[11] Other characteristic bands in the spectra of PDMAEMA_AIBN and PDMAEMA_ACVA appeared at 2951 and 2953 cm^{-1}, respectively, attributed to C–H stretching of methyl and –CH2– groups. The absorption bands in the 2818-2772 cm^{-1} domain were assigned to C–H stretching vibration of –N(CH3)2 group.[11, 12] In addition, characteristic peaks of –CH2– bending and C–N stretching vibrations were identified in the PDMAEMA_AIBN and PDMAEMA_ACVA FTIR spectra at 1458 cm^{-1} and 1153 cm^{-1}, respectively. By comparison, the spectrum of PDMAEMA homopolymer prepared in distilled water by using the KPS/AscA redox initiation system presented not only characteristic peaks of PDMAEMA (2976-2885 cm^{-1} - C–H stretching vibration, 1726 cm^{-1} - stretching vibration of C=O group, 1475cm^{-1} – CH_3 anti-symmetric bending, 1362 cm^{-1} – CH_3 symmetric bending 1269 cm^{-1} – C-O-C anti-symmetric stretching, 1169 cm^{-1} -C–O-C symmetric stretching), but also new absorption bands: at 3479 cm^{-1} assigned to O-H stretching vibration of adsorbed water molecules and hydrophilic end groups of the homopolymer derived from initiators and at 1593 cm^{-1} which may result from the coordination of the free electron pair of the tertiary amino group with the carboxyl from DMAEMA.[13]

^{1}H-NMR Spectroscopy

Figure 2 shows ^{1}H-NMR spectra of the synthesized PDMAEMA homopolymers in D_2O under acidic (pH 1) conditions. The signals between 0.92-1.05 ppm in Figure 2 are assigned to the methyl protons and the peaks between 1.85-2.0 ppm are attributed to the methylene protons in the polymer backbone. Also, the signals at 4.2 ppm, 2.8-2.98 ppm and 2.3-2.5 ppm were assigned to the two methylene protons(s, 2H, O—CH2—; s, 2H, —CH2—N) [14] and six terminal methylene protons of the DMAEMA units (s, 6H,—N—$CH_3)_2$), respectively.

Additionally, in the ^{1}H-NMR spectrum of PDMAEMA_KPS/AscA appeared new peaks in the intervals 3.29-3.4 ppm and 3.89-3.95 ppm, respectively, which are assigned to the initiator fragments (ascorbate radicals).[15]

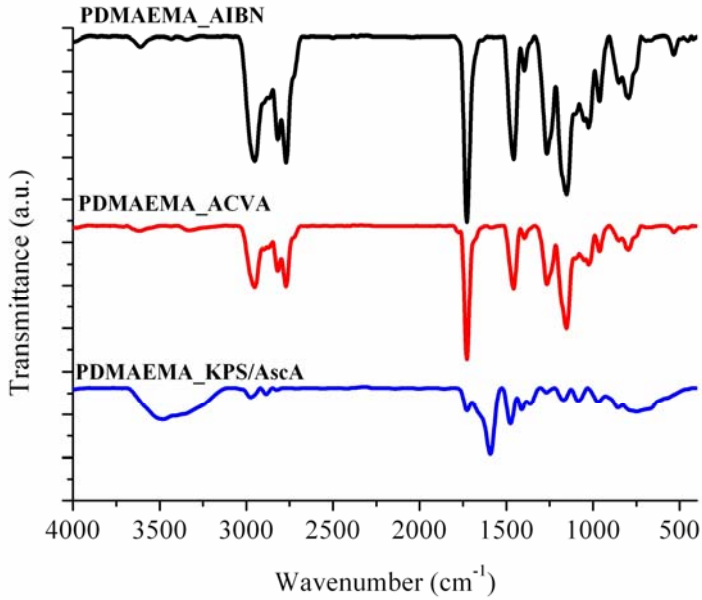

Fig. 1 – FTIR spectra of the synthesized PDMAEMA homopolymers accordingly with the synthesis variant.

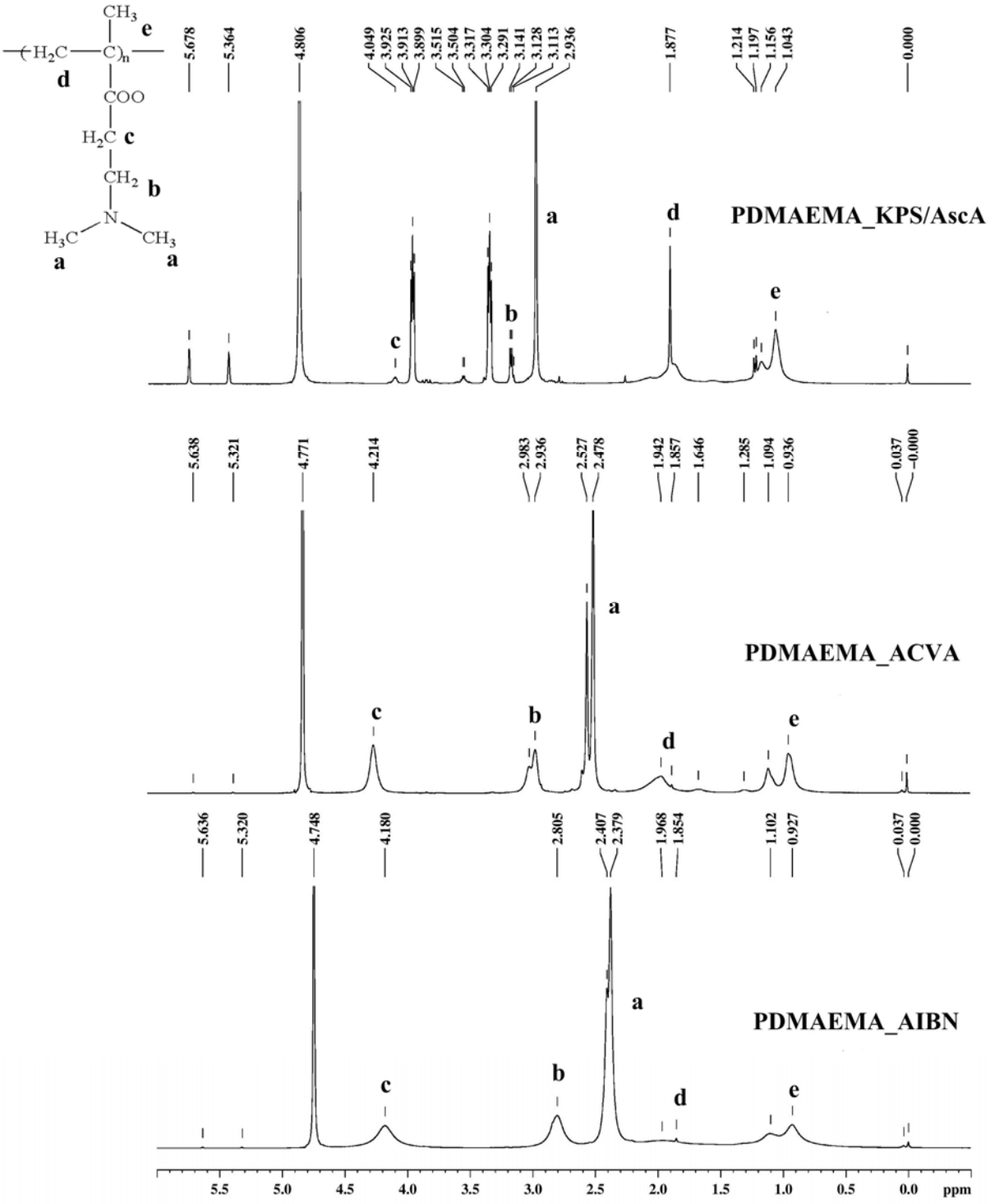

Fig. 2 – ^{1}H-NMR spectra of the synthesized PDMAEMA homopolymers accordingly with the synthesis variant.

DLS and SLS investigation for molecular weight and LCST evaluation

The molecular weight and the second virial coefficient (A_2) of the synthesized homopolymers were determined using the Zetasizer NanoS system. The static light scattering technique (SLS) was used for measuring the molecular weight of PDMAEMA at only one angle (173°) by using Rayleigh equation (eq. 1) that describes the relation between the intensity of the scattered light of macromolecules and their gravimetric average molecular weight (M_w). The study evidences the interdependence between the initiator type (the

reaction conditions) and the molecular weight of the synthesized PDMAEMA homopolymers. A specific molecular weight for the macromolecular chains influences not only the physico-chemical properties of the compound but also the further applicability of the polymer. The slope of KC/R_θ plot versus C for $\theta \rightarrow 0$ with the intercept equivalent to 1/M gives the value of the second virial coefficient (A2). The molecular weight is determined as the intercept of the plot of KC/R_θ versus C from the equation:

$$\frac{KC}{R_\theta} = (\frac{1}{M_w} + 2A_2C)P(\theta) \quad (1)$$

in which K - the optical constant and P(θ) - the shape factor are given as:

$$K = \frac{2\pi^2}{\lambda_0^4 N_A}(n_0 \frac{dn}{dc})^2 \quad (2)$$

$$P_\theta = 1 + \frac{16\pi^2 n_0^2 Rg^2}{3\lambda_0^2}\sin(\frac{\theta}{2}) \quad (3)$$

and

$$R_\theta = \frac{I_A n_0^2}{I_T n_T^2} R_T \quad (4)$$

where: M_w is the gravimetric average molecular weight, A_2 is the second virial coefficient, C is polymer concentration, R_θ is the Rayleigh ratio of the scattered to incident light intensity, n_o is the refractive index of the solvent, the laser wavelength, N_A is the Avogadro constant, and dn/dc is the refractive index increment of the scattering species in the solvent used. Also, R_g is the radius of gyration, θ represents the measurement angle, I_A is the intensity of sample, I_T is the intensity of standard (toluene), n_T is the standard toluene refractive index and R_T is the Rayleigh ratio of standard (toluene).

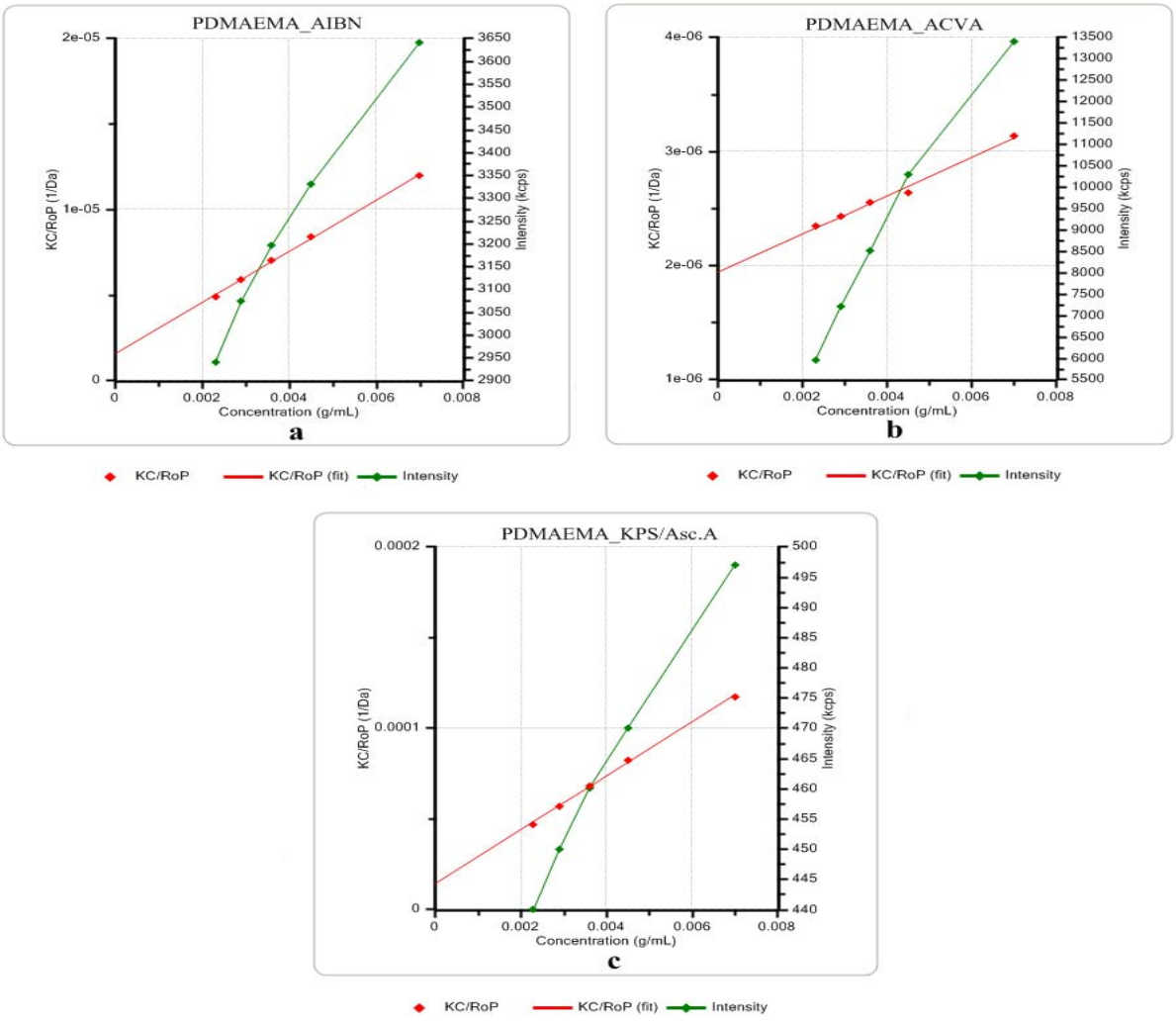

Fig. 3 – Debye plots for a) PDMAEMA_AIBN, b) PDMAEMA_ACVA and c) PDMAEMA_KPS/AscA.

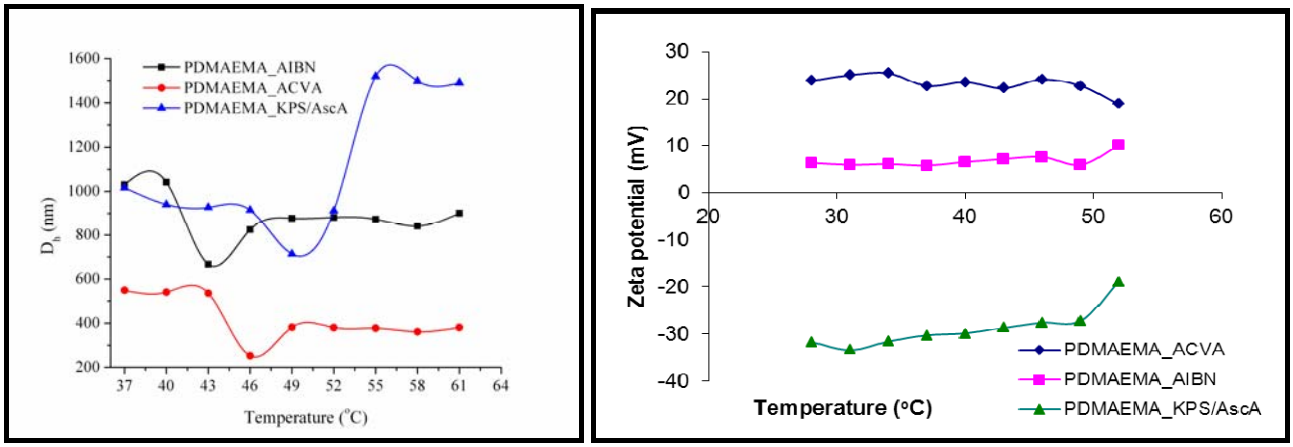

a **b**

Fig. 4 – Variation of hydrodynamic diameter (a) and zeta potential (b) with temperature for the synthesized homopolymers in relation with the initiation variant.

The data resulted from SLS measurements evidenced (Figure 3) that the gravimetric molecular weights of PDMAEMA_AIBN (644.1±52.5 kDa) and PDMAEMA_ACVA (516.5±12.2 kDa) were much higher than that of PDMAEMA homopolymer synthesized by the redox initiation system (71.1±7.0 kDa). Accordingly to the redox process developed by the potassium persulfate / ascorbic acid system, two active species[16] are able to initiate the polymerization reactions (Table 1) namely ascorbate and sulphate ion radicals. In this case, a diminished molecular weight was obtained as a result of the increased radical decomposition rate induced by the higher polymerization temperature. Also, a slight difference was registered between the molecular weights of PDMAEMA_AIBN and PDMAEMA_ACVA, which can be justified by the fact that AIBN has a slight lower decomposition rate (k_d=3.2 x 10^{-5} s^{-1} in toluene at 70°C[16]) compared with ACVA initiator (k_d=4.6 x 10^{-5} s^{-1} in acetone at 70°C[17]).

The shape of the hydrodynamic diameter evolution is specific for each variant of homopolymer, as can be seen from Figure 4a. At the same time it must notice some similarities between the behavior of the PDMAEMA variants initiated by the azo-initiators. The fact was attributed to the influence of the radical initiator presence at the end of the macromolecular chains, which induces the behavior of the macromolecules in interdependence with the environmental conditions as temperature, pH, or the presence of ions. It must also evidence a re-phasing of the temperature correspondingly to the minimum value for D_h particles of PDMAEMA_AIBN (43°C) and that of PDMAEMA_ACVA (46°C) respectively.

At the beginning of the investigation temperature, all the homopolymer samples present a decrease in D_h, followed by a sudden increase in the hydrodynamic diameter that started at 44°C (PDMAEMA_AIBN), 47°C (PDMAEMA_ACVA) and 51°C (PDMAEMA_KPS/AscA) (Figure 4). The decrease in D_h was attributed to a gradual decrease in the affinity of the polymer coils towards buffer solution, while the increase was attributed to the collapse of polymer coils leading to aggregation.[11] Moreover, the nature of the end groups derived from the used system of initiation is modifying the hydrodynamic diameter trend of the homopolymers, by changing the hydrophobic/hydrophilic nature of them.[18] Therefore, as it can be observed from Figure 3a, the hydrophilic end groups of PDMAEMA_KPS/AscA induced not only an increase of the LCST, but also an increase of the hydrodynamic diameter.

The influence of the end groups of the macromolecular chains, derived from the nature of the initiators, is also confirmed by the zeta potential values registered during DLS investigation. Therefore, different data of zeta potential correspond in relation with the system of initiation, respectively negative values and much higher in the case of PDMAEMA_KPS/AscA variant (up to 33.4 in modulus) and positive and lowest values for PDMAEMA_AIBN (up to 10).

Thermal analysis

The thermal degradation data (TGA and Gram Schmidt-GS) of the compounds are summarized in Table 2. In the case of PDMAEMA_AIBN and PDMAEMA_ACVA, the thermal degradation process occurred in three stages, with different weight loss at every stage of decomposition.

Table 2

The main thermogravimetric parameters

Sample	Degradation stage	T_{onset} °C	T_{peak} °C	W %	T_{10} °C	T_{20} °C	GS °C
PDMAEMA_AIBN	I	219	251	6.27	282	310	251
	II	301	318	35.83			317
	III	381	414	42.84			415
	residue			15.06			
PDMAEMA_ACVA	I	225	263	5.18	298	312	264
	II	300	317	38.69			317
	III	378	413	40.35			421
	residue			15.78			
PDMAEMA_KPS/AscA	I	42	-	2.50	157	185	182
	II	123	182	29.47			261
	III	233	260	29.97			414
	IV	383	417	28.32			
	residue			9.74			

Instead, PDMAEMA_KPS/AscA exhibited four distinct weight loss steps, with the first stage being attributed to the loss of bound water. According to the TGA results, in the first degradation stage of PDMAEMA_AIBN and PDMAEMA_ACVA, T_{onset} varies between 219°C and 225°C (Table 2) and mass losses were about 6.27% and 5.28%. This stage could be attributed to the decomposition and loss of the end groups alone, as reported in the literature.[19] In the second stage of PDMAEMA_AIBN and PDMAEMA_ACVA degradation, T_{onset}, is around 300°C and weight loss are between 35.83 and 38.68%; this stage may be characteristic to the removal of dimethylaminoethyl groups. The increasing of the heating temperature above 300°C leads to a new stage of degradation with weight losses ranging between 42.84 and 40.35%. This final stage of degradation is a result of the thermal decomposition of polymer backbones and the releases of saturated or unsaturated aliphatic fragments of higher molecular weights,[20,21] CO and CO_2[19] highlighted by mass spectrometry/FTIR spectroscopy coupled online with thermogravimetric balance. Additionally, the char values indicated that PDMAEMA_KPS/AscA is less stable than PDMAEMA_AIBN and PDMAEMA_ACVA that were synthesized via AIBN and ACVA radical initiation, which is in good agreement with the molecular weight of the homopolymer.

Because all the samples presented similar TG curves profiles, PDMAEMA_AIBN homopolymer was selected to be studied from the point of view of its thermal decomposition mechanism using TG analyzer connected on-line with the FTIR spectrophotometer and mass spectrometer (TGA-FTIR-MS), on the 30°C -600°C temperature range. In Figure 5a it is illustrated the 3D FTIR spectrum of the PDMAEMA_AIBN evolved gases. The thermal degradation of PDMAEMA_AIBN homopolymer, as TG analysis revealed, followed three stages. The evolved gases were identified using the IR spectra and MS signals database, available in the spectral libraries of the NIST.[20] The 2D FTIR spectra attributed to the gaseous byproducts released at temperatures of 251, 318 and 415°C were extracted from 3D FTIR spectrum of PDMAEMA_AIBN (Figure 5b).

The FTIR spectra of the evolved gases recorded during the first weight loss showed bands at 2952 and 2789 cm^{-1} attributed to C–H stretching vibrations for methyl and methylene groups from aliphatic groups, 2360 cm^{-1} – CO_2, 1282 cm^{-1}, 1169 cm^{-1} assigned to C–O and C–N stretching vibrations of the ester and aliphatic amine groups and 1038 cm^{-1} attributed to C–O–C vibration. The appearance of an absorption peak at 1649 cm^{-1}, attributed to C=C stretching, may correspond to a double bond that is formed after the cleavage of the ester group of PDMAEMA_AIBN (CH2=CH-N(CH3)2). The absorption bands in the 2700-3200 cm^{-1} domain, corresponding to C-H stretching, gradually decrease as the thermal degradation process continues. Additionally, as mass loss increases, it can be observed that the 2360 cm^{-1} band characteristic to CO_2 significantly increases, suggesting a pronounced carbonization processes that takes place in the last stage of PDMAEMA_AIBN thermal decomposition.

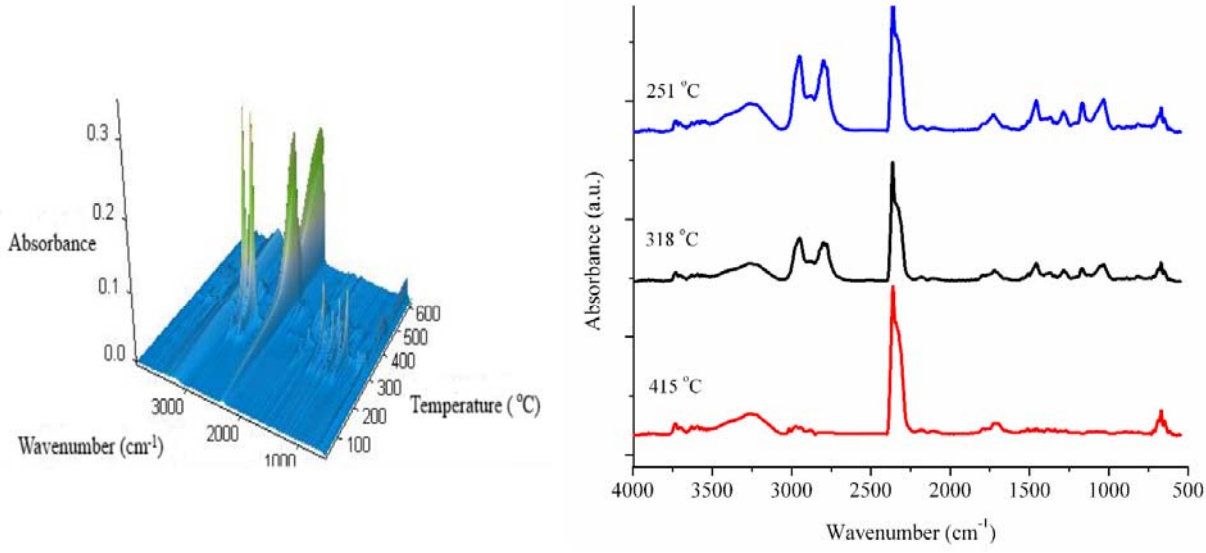

a **b**

Fig. 5 – 3D (a) and 2D (b) FTIR spectra of the evolved gases following thermal decomposition of PDMAEMA_AIBN.

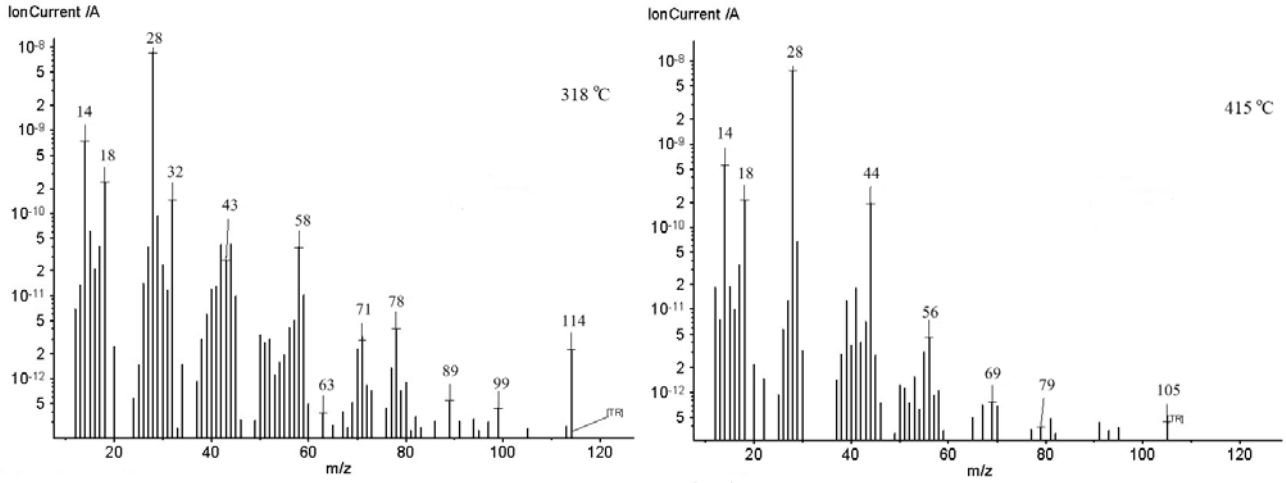

a **b**

Fig. 6 – MS spectra of ionic fragments released during thermal decomposition of PDMAEMA_AIBN at: a) 318°C and b) 415°C.

The identification of the volatile compounds that results from the thermal degradation of PDMAEMA_AIBN was performed using the NIST data base.[22] The mass spectra of volatile products at 318°C and 415°C where the maximum amounts of gases are released are given in Figure 6. These signals can be associated with the ester groups' cleavage and chains scission resulted following thermal decomposition. Other processes that occur at high temperatures are fragmentation or recombination reactions. Taking into account the above mentioned results, it is possible to presume that the main volatile products released during thermal degradation of PDMAEMA_AIBN were CO^+ or $C_2H_4^+$ (m/z=28), $C_2H_4N^+$ (m/z=42), $C_4H_9N^+$ (m/z=72), $C_4H_8^+$ (m/z=56), $C_5H_9^+$ (m/z=69), C_6H_5+2H (m/z=79), C_6H_5-C=O^+ (m/z=105). The release of carbon dioxide during thermal degradation was confirmed by a fragment at *m/z* 44 (CO_2^+), an observation that is also sustained by FTIR spectra where carbon dioxide has been observed in all the three stages.

Dielectric properties of PDMAEMA homopolymers

The dielectric permittivity is a complex parameter that could be expressed as:

$$\varepsilon^* = \varepsilon' - i\varepsilon'' \quad (5)$$

where ε' is the dielectric constant that is related to the capability of dipolar groups to follow an alternative field, and ε" is the dielectric loss that is related to the dissipated energy required to align the dipoles. In this section, the evolution of ε' and ε" with temperature and frequency is investigated. The behavior of dielectric constant with temperature, at various frequencies, is represented in Figure 7. At low temperatures (-150°C – -50°C), the chemical groups absorb a small quantity of thermal energy and, as consequence, ε' increases slightly and linearly with temperature. With further increasing in temperature, ε' increases considerably because the polarizable units gain enough thermal energy and might easier orient in the direction of the applied field. This aspect is displayed in the 70 – 100°C temperature interval. The ordinary evolution of dielectric constant is modified by an uncommon and very intense peak, in the -50 – 70°C range. This non-dielectric peak is specific to a possible physical process, generally associated with water molecules and/or solvent traces that might be included in the bulk material. Moreover, the temperature characteristics are displayed at different frequencies (1Hz, 10Hz, 10^2Hz, 10^3Hz, 10^4Hz, 10^5Hz and 10^6Hz, respectively). According to Figure 7, at low frequencies, the dipolar groups have enough time to follow external field, while at high frequencies the dipoles rotates within small angle and, as consequence, the magnitude of ε' decreases considerably as frequency increases from 1Hz to 10^6Hz.[23, 24]

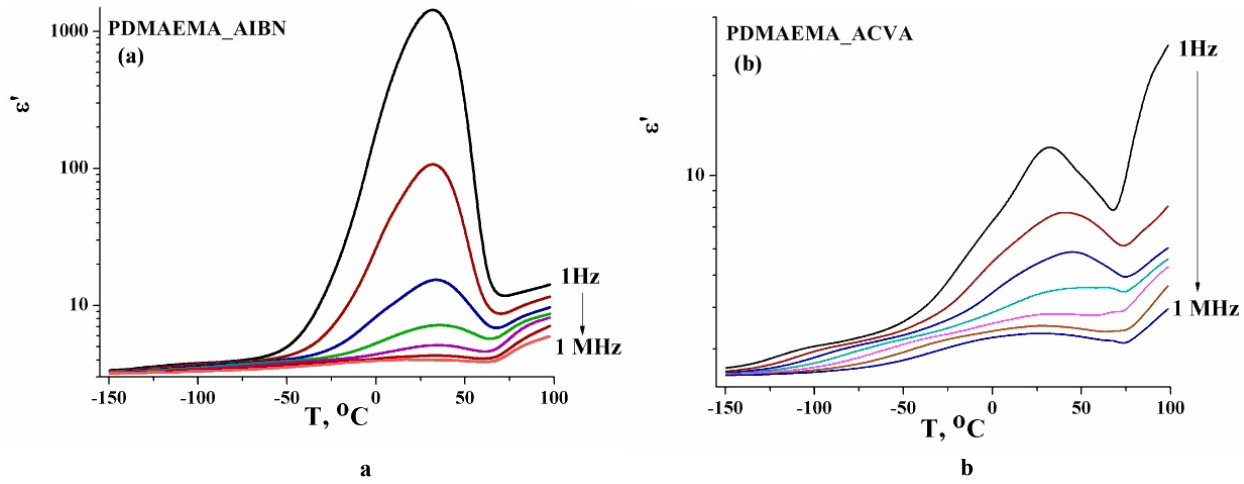

Fig. 7 – Dielectric constant evolution with temperature at different frequencies for AIBN (a) and ACVA (b) samples.

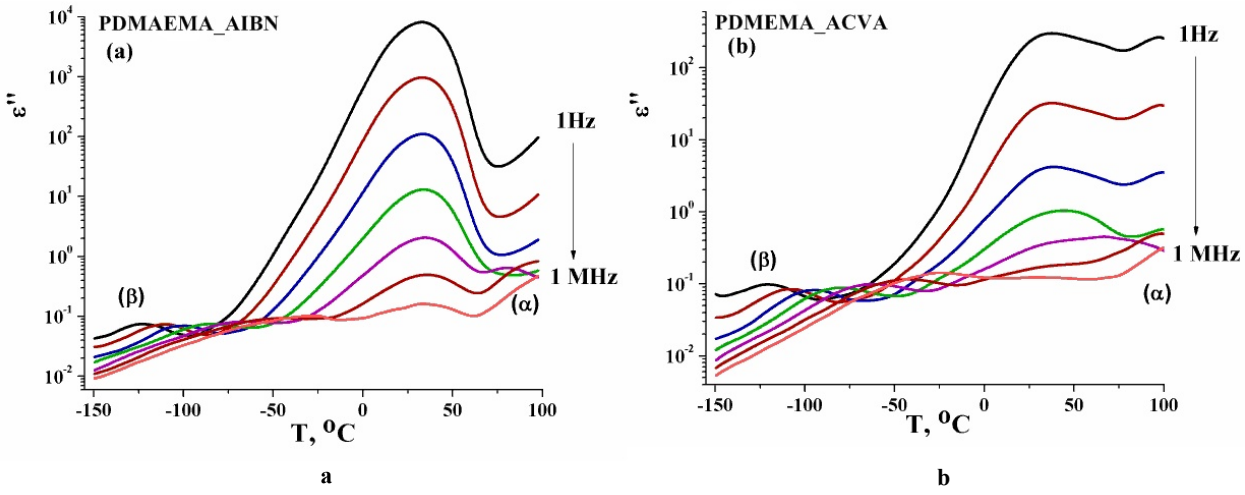

Fig. 8 – The temperature evolution of dielectric loss at different frequencies for PDMAEMA_AIBN (a) and PDMAEMA_ACVA (b) samples.

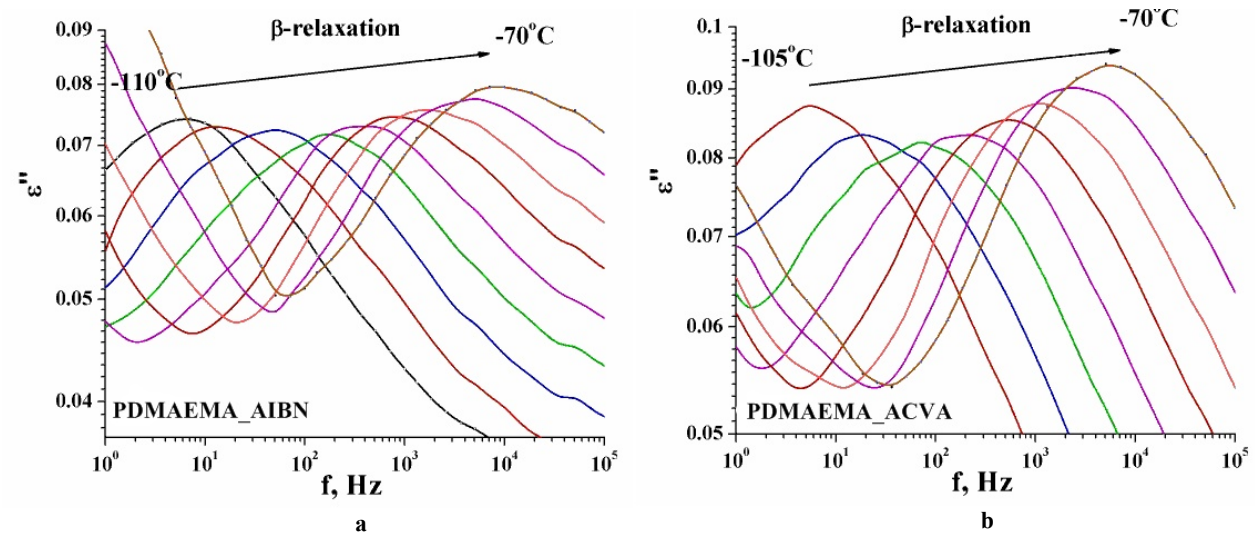

Fig. 9 – ε”(f) dependencies of β-relaxation for a) PDMAEMA_AIBN and b) PDMAEMA_ACVA samples.

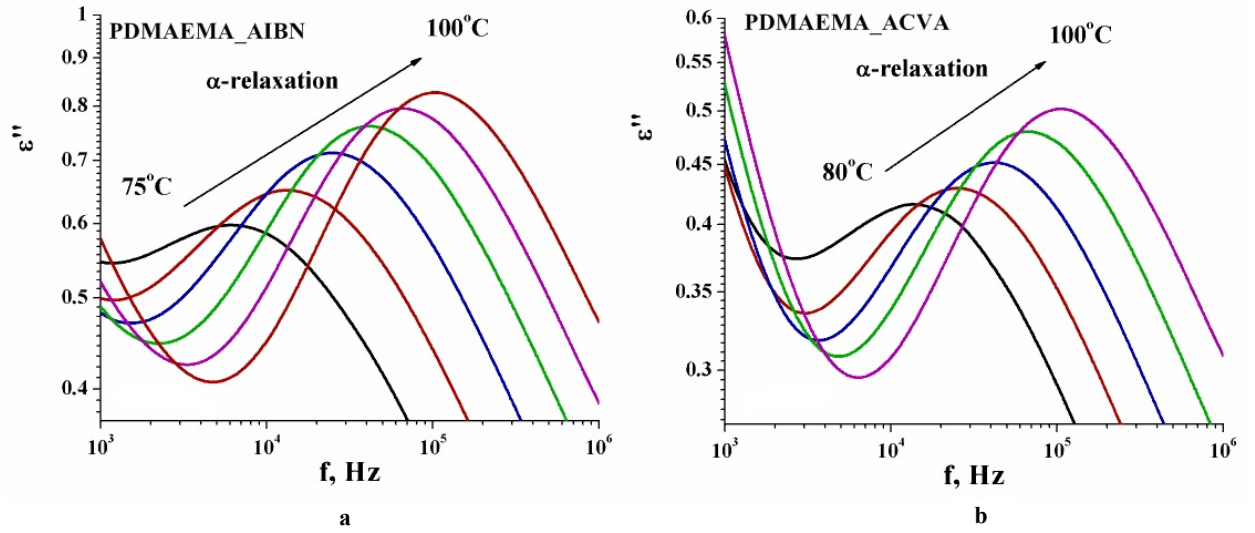

Fig. 10 – ε”(f) dependencies of α-relaxation for a) PDMAEMA_AIBN and b) PDMAEMA_ACVA samples.

The temperature evolution of dielectric loss for different frequencies, represented in Figure 8, reveal the existence of relaxation-type dipolar processes. Generally for both samples, at low temperatures (-120°C– -30°C) β-relaxation is recognized as a well-defined peak that shifts its position at higher temperatures as frequency increases (e.g. for f=10Hz, β-relaxation is detected at -110°C). At high temperatures (75°C–100°C), α-relaxation connected to glass transition is observed only at high frequencies (at low frequencies the conductivity signal is significant and covers the primary dielectric signal).

The ε”(f) dependencies β- and α-relaxations for both samples are revealed in Figure 9 and Figure 10. According to these frequency spectra, the dipolar relaxations appears as well-shaped peaks that moves toward temperature, providing that these processes are thermally activated.

The dipolar relaxations are better emphasized on 3d version of dielectric loss function of frequency and temperature (Figure 11). β – relaxation is localized at low temperatures, while at further increase in temperature, α - relaxation connected to glass transition is recognized only at high frequencies, as a shoulder strongly overlapped by conductivity signal.

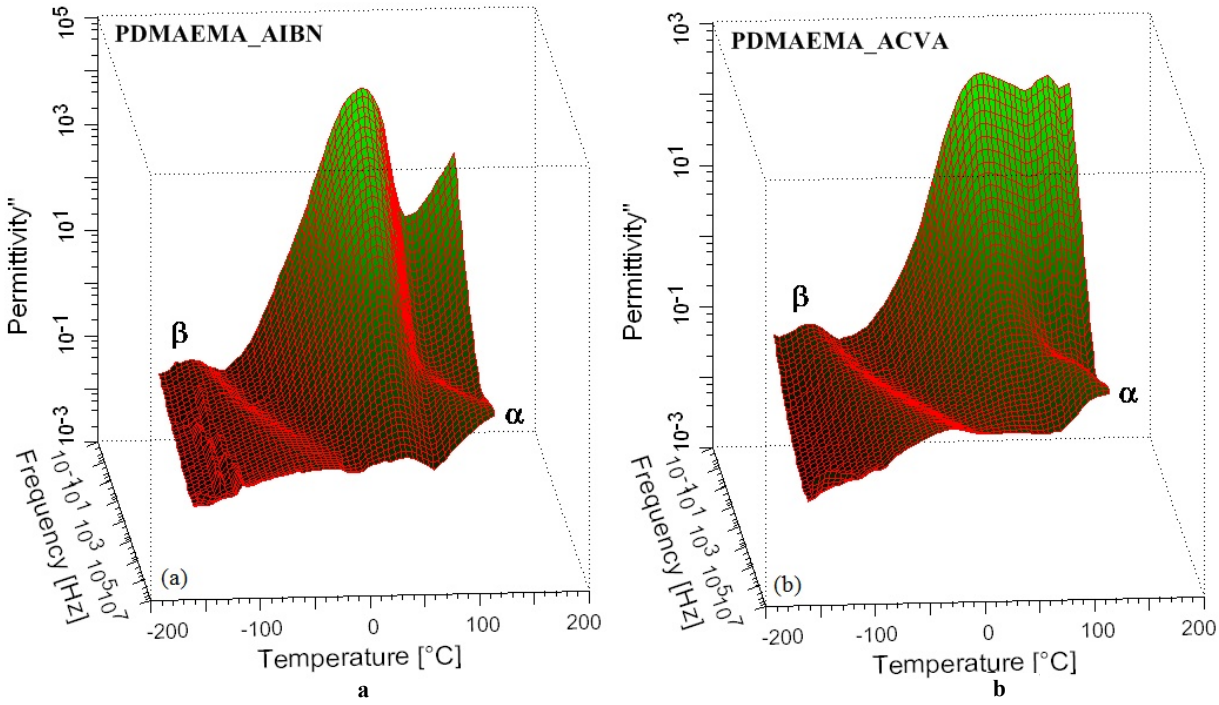

Fig. 11 – Evolution of dielectric loss with frequency and temperature for a) PDMAEMA_AIBN and b) PDMAEMA_ACVA samples.

Furthermore, each ε"(f) dependency has been processed with the WinFit software package in order to determine the activation energy of the dipolar processes. For this purpose, the Havriliak-Negami (HN) formula has been considered:

$$\varepsilon^* = \varepsilon' - \varepsilon'' = \varepsilon_u + \frac{\varepsilon_r - \varepsilon_u}{[1+(i\omega\tau_{HN})^a]^{b'}} \qquad (6)$$

where ε_r and ε_u are the relaxed ($\omega \to 0$) and unrelaxed ($\omega \to \infty$) values of the dielectric constant, τ_{HN} is the HN relaxation time for the process, a and b represent the broadening and skewing parameters, respectively.[24, 25]

Examples of HN fitting process are displayed in Figure 11 for PDMAEMA_ACVA sample (β-relaxation in Figure 11a and α-relaxation in Figure 12b). ε"(f) dependencies are processed with a HN function specific to the dielectric process and a function specific to the conductivity (green lines). The sum of the HN function and the conductivity term is displayed with the blue line and correspond to the experimental points, presented with red.

The activation energy, E_a, of a dipolar process is associated with the rotation of dipoles in the direction of an applied field. It is, thus, connected to the potential energy barrier of the fluctuated dipolar molecules. Related to our results, at low temperatures (-120°C – -30°C), where the dipoles absorb a small quantity of thermal energy, only restricted number of chemical groups is activated. The process, known as to β-relaxation, is produced by local movements of chemical groups from side chain macromolecules without disturbing the main chain (e.g. polar carbonyl R-C=O groups from the side part of macromolecular chain, or polar amine from dimethylaminoethyl side). At high temperatures around the glassy state, the thermal energy earned by polar groups is substantial and the primary α-relaxation is activated.[26] The dipolar process is produced by movements of large segments, even from the main chain (e.g. polar ether group from methacrylate).

Figure 13 shows the relaxation times versus reciprocal temperatures in Arrhenius-type representation for β - and α - relaxation processes. Similar characteristics and similar activation energies as well, are observed, suggesting that the same processes occur in both samples.

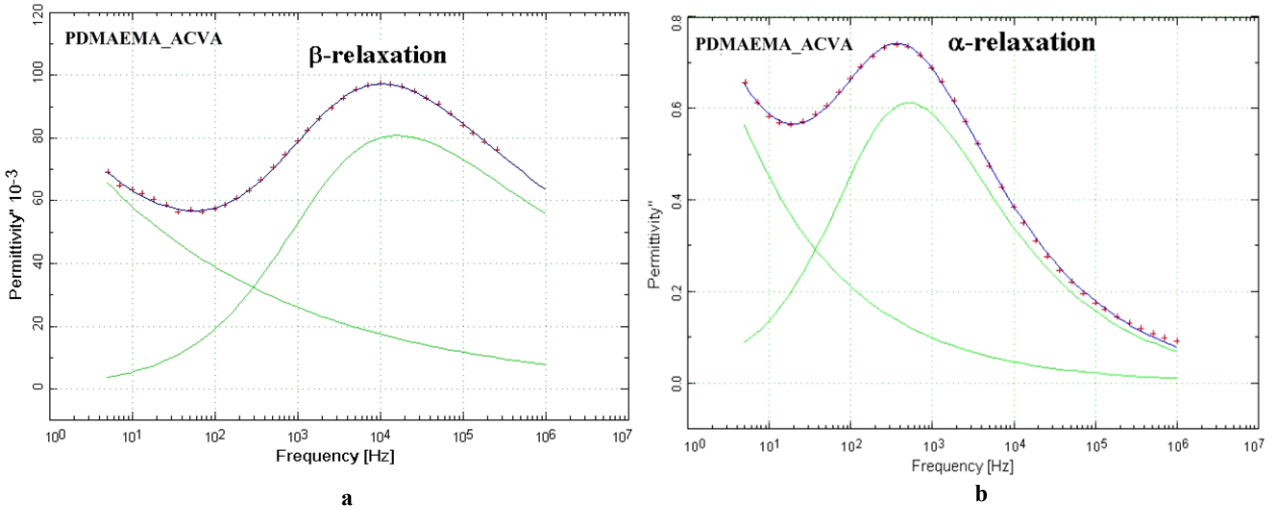

Fig. 12 – Examples of HN fitting process for a) β-relaxation and b) α-relaxation of PDMAEMA_ACVA sample.

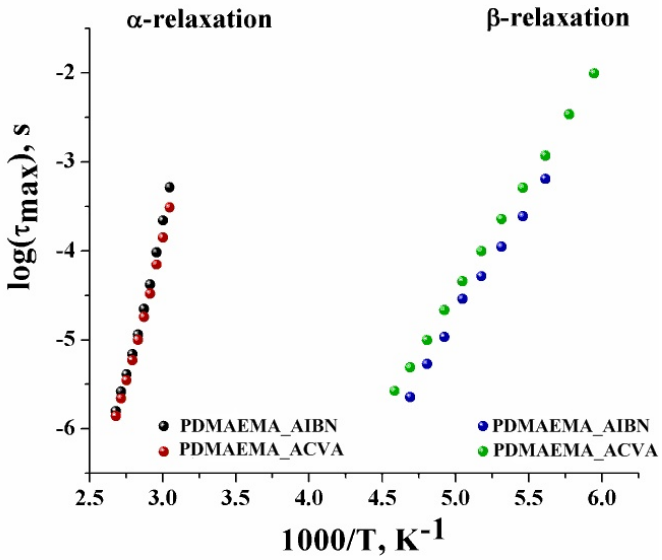

Fig. 13 – Arrhenius type representation for α - and β – relaxation.

EXPERIMENTAL

Materials

All the reagents were of analytical purity and were used without further purification: 2,2′-Azobis(2-methyl-propionitrile) (AIBN) (purity 98 %, Sigma-Aldrich), 4,4′-Azobis(4-cyanovaleric acid) (ACVA) (75% purity, Aldrich), potassium persulfate (KPS) (99.99% trace metals basis, Aldrich), L-ascorbic acid (AscA) (Sigma), tetrahydrofuran (99.9% purity, Sigma-Aldrich). Only 2-(dimethylamino) ethyl methacrylate (DMAEMA) (Alfa Aesar) was purified prior to the polymerization process by passing through an inhibitor removal column.

Preparation of poly(2-(dimethylamino) ethyl methacrylate) (PDMAEMA)

The homopolymers were synthesized by free radical polymerization of DMAEMA using various systems of initiation: a) AIBN (k_d (s^{-1}) = 3.2 x 10^{-5}), b) ACVA (k_d (s^{-1}) = 4.6 x 10^{-5}) and c) a redox system composed from KPS and AscA. In the case of PDMAEMA_AIBN and PDMAEMA_ACVA synthesis, the polymerization reactions were conducted in tetrahydrofuran (THF). For PDMAEMA_KPS/AscA preparation, the free radical polymerization was performed in bidistilled water. All reactions were carried out at 70°C for 20 h, keeping the same proportion of reactants. The systems were flushed with nitrogen for approximately 5 min. before starting the reaction. The obtained homopolymers variants were purified by the three-phase partitioning (TPP) technique, an efficient technique mostly used for protein and enzyme separation.[27, 28] As it is specified in the literature, the precipitated compound accumulates at the interface between an organic liquid phase and an aqueous solution of a salting out salt, forming a third phase.[29] NaCl supersaturated solution was used for PDMAEMA purification.

Methods of characterization

Fourier Transform Infrared (FTIR) spectra of the PDMAEMA homopolymers have been obtained using a

Vertex Brucker Spectrometer in the transmittance mode ranging from 400 to 4000 cm^{-1}.

Proton Nuclear Magnetic Resonance (^1H NMR) spectra were recorded on a Bruker Avance DRX400 NMR spectrophotometer Rheinstetten (Germany) with 16 scans and 0.1 Hz.

Dynamic light scattering (DLS) and static light scattering (SLS) analysis. In order to analyze the molecular weight, SLS measurements of the PDMAEMA homopolymers in 3M HCl solutions at 2.3–7.0 mg/ml was performed, and a Debye plot was represented using the scattering intensity. In order to evaluate the LCST of PDMAEMA homopolymer at different temperatures, aqueous buffer solutions of the polymer samples were subjected to analysis through DLS using a Zetasizer model Nano ZS device, with red laser 633 nm He/Ne from Malvern Instruments, UK. The hydrodynamic diameter (D_h) of the sample was measured in aqueous solution at pH 8.0 and temperatures between 25°C and 60°C. The zeta potential values of the PDMAEMA_AIBN, PDMAEMA_ACVA, PDMAEMA_KPS/AscA samples were evaluated also in aqueous solution at pH 8.0 and the temperature range between 28°C up to 55°C. According to literature, at pH 8.0 PDMAEMA exhibits enough hydrophobic features to cause the occurrence of LCST.[11]

Thermogravimetric analysis (TGA) coupled with FTIR and mass spectrometry (MS). The thermal behavior of samples was investigated by *thermogravimetric analysis (TGA).* The measurements were performed on a STA 449F1 Jupiter (Netzsch, Germany) type derivatograph (thermogravimetric analyzer). The thermal decomposition of PDMAEMA_AIBN, PDMAEMA_ACVA, PDMAEMA_KPS/AscA and evolved gas analyses were carried out using three different coupled techniques: TGA coupled with FTIR and mass spectrometry (MS).

Dielectric spectroscopy. Complex dielectric permittivity measurements were realized using the Novocontrol Dielectric Spectrometer (GmbH Germany), CONCEPT 40 in the range of frequency (1–10^6 Hz) and temperature (−150–120°C), in nitrogen atmosphere avoiding water absorption.

CONCLUSIONS

In this study, PDMAEMA was obtained by free radical polymerization of DMAEMA using various systems of initiation. At pH 8, PDMAEMA exhibited a thermo-responsive behavior and the LCST values were in the range of 44°C and 51°C. The results were consistent with previously published LCST values for PDMAEMA. The study of PDMAEMA using the online TG-FTIR-MS technique provided more specific information about the thermal decomposition process and the evolved gaseous products. PDMAEMA_AIBN and PDMAEMA_ACVA underwent thermal decomposition under nitrogen atmosphere in three stages, but PDMAEMA_KPS/AscA degradation occurred in four stages. In the first stage the main process was the cleavage of ester linkages with the formation of alcohols and both saturated and unsaturated tertiary amines. The evaluation of the dielectric properties of PDMAEMA_AIBN and PDMAEMA_ACVA showed that β-relaxation is localized at low temperatures, while at further increase in temperature, α-relaxation is recognized only at high frequencies. In conclusion, as o consequence of its non-degradable nature, increased thermal stability and large molecular weight, PDMAEMA_AIBN and PDMAEMA_ACVA homopolymers can be used to synthesis wound dressings or scaffolds for tissue engineering applications that require thermal sterilization. Instead, PDMAEMA_KPS/AscA can be used in the preparation of polymeric carriers because its low molecular weight will allow the elimination from the human body through the renal clearance.

Acknowledgments: This work was financially supported by the grant of the Roumanian National Authority for Scientific Research, CNCS-UEFISCDI, project number PNII-RU-TE-2014-4-0294 „Novel hydrogels synthesis with defined 3D functionality and biodegradable characteristics for bioapplications".

REFERENCES

1. T. Celik and N. Orakdogen, *Macromol. Chem. Phys*., **2015**, *216*, 2190-2201.
2. N. Orakdogen, *J. Polym. Res.*, **2012**, *19*, 9914
3. E. Dragan, D. Apopei Loghin, A. Cocarta and M. Doroftei, *React. Funct. Polym.*, **2016**,*105*, 66-77.
4. C. Gao, M. Liu, J. Chen and C. Chen, *J. Biomat. Sci.-Polym. E*., **2012**, *23*, 1039-1054.
5. B. Horev, M. Klein, G. Hwang, Y. Li, D. Kim, H. Koo and D. Benoit, *ACS Nano.,* **2015**, *9*, 2390-2404.
6. C. Gao, M. Liu, S. Chen, S. Jin and J. Chen, *Int. J. Pharm*., **2009**, *371*, 16-24.
7. E. Adolph, C. Nelson, T. Werfel, R. Guo, J. Davidson, S. Guelcher and C. Duvall, *J. Mater. Chem. B*, **2014**, *2*, 8154-8164.
8. S. Chen, J. Li, T. Pan, P. Li and W. He, *Polymers*, **2016**, *8*, 38.
9. Y. You, D. Manickam, Q. Zhou and D. Oupický, *J. Control. Release*, **2007**, *122*, 217-225.
10. F. Zeng, Y. Shen, S. Zhu and R. Pelton, *J. Polym. Sci. A Polym. Chem.*, **2000**, *38*, 3821-3827.
11. L. Bonkovoski, A. Martins, I. Bellettini, F. Garcia, C. Nakamura, A. Rubira and E. Muniz, *J. Control. Release*, **2015**, *213*, e29-e30.
12. D. Roy, J. Guthrie and S. Perrier, *Soft Matter*, **2008**, *4*, 145-155.
13. C. Li, G. Wang, H. Gao, M. Zhai and J. Li, *J. Appl. Polym. Sci*, **2013**, *131*.
14. R. Reid, *J. Chem. Educ.*, **1989**, *66*, 344.
15. G. Gao, M. Karaaslan and J. Kadla, *Macromol. Mater. Eng.,***2014**, *299*, 990-1002.

16. G.S. Misra and C.V. Gupta, *Makromol. Chem.*, **1973**, 165, 205-211.
17. J. Brandrup, E.H. Immergut and E.A Grulke, "Polymer Handbook", John Wiley, 4th Edition, 1999.
18. Y. Xia, X. Yin, N. Burke and H. Stöver, *Macromolecules*, **2005**, *38*, 5937-5943.
19. S. Roy, K. Bauri, S. Pal, A. Goswami, G. Madras and P. De, *Polym. Int*., **2012**, *62*, 463-473.
20. N. Tudorachi and A. Chiriac, *Polym. Test*., **2011**, *30*, 397-407.
21. J. Chen, P. Xiao, J. Gu, Y. Huang, J. Zhang, W. Wang and T. Chen, *RSC Adv.,* **2014**, *4*, 44480-44485.
22. Information on http:// webbook.nist.gov/ chemistry/name-ser.html].
23. S. Bronnikov, S. Kostromina, V. Musteaţa and V. Cozan, *Liq. Cryst*., **2015**, *42*, 1102-1110.
24. S. Chisca, V.E. Musteata, I. Sava and M. Bruma, *Eur. Polym. J.,* **2011**, *47*, 1186–1197.
25. S. Havriliak and S. Negami, *Polymer,* **1967**, *8*, 161-210.
26. S. Bronnikov, A. Podshivalov, S. Kostromin, M. Asandulesa and V. Cozan, *Eur. Polym. J*., **2016**, *78*, 213–225.
27. R. Pike and C. Dennison, *Biotechnol. Bioeng*., **1989**, *33*, 221-228.
28. B. Paule, R. Meyer, L. Moura-Costa, R. Bahia, R. Carminati, L. Regis, V. Vale, S. Freire, I. Nascimento, R. Schaer and V. Azevedo, *Protein Expr. Purif.*, **2004**, *34*, 311-316.
29. T. Przybycien, N. Pujar and L. Steele, *Curr. Opin. Biotechnol*., **2004**, *15*, 469-478.